Theoretical study of the Ti-Cl bond cleavage reaction in TiCl$_4$

Daniel Nurkowski[1], Ahren W. Jasper[2], Jethro Akroyd[1], Markus Kraft[1,3]

released: 09 November 2016

[1] Department of Chemical Engineering
and Biotechnology
University of Cambridge
New Museums Site
Pembroke Street
Cambridge, CB2 3RA
United Kingdom
E-mail: mk306@cam.ac.uk

[2] Sandia National Laboratories
Livermore, CA 94551-0969
E-mail: ajasper@sandia.gov

[3] School of Chemical
and Biomedical Engineering
Nanyang Technological University
62 Nanyang Drive
Singapore 637459

Preprint No. 175

UNIVERSITY OF
CAMBRIDGE

Edited by
Computational Modelling Group
Department of Chemical Engineering and Biotechnology
University of Cambridge
New Museums Site
Pembroke Street
Cambridge CB2 3RA
United Kingdom

Fax: + 44 (0)1223 334796
E-Mail: c4e@cam.ac.uk
World Wide Web: http://como.cheng.cam.ac.uk/

Highlights

- A detailed theoretical study of the rate of the $TiCl_3$ + Cl reaction is presented.
- Variable-reaction coordinate transition-state theory is combined with the master equation to estimate the rate coefficients at various pressures and temperatures.
- Multireference CASPT2(6e,4o)/cc-pVDZ level of theory is employed to dynamically build the reactive surface.
- Collisional energy transfer parameters for $TiCl_4$–Ar system are estimated using a "one-dimensional minimisation" and classical trajectories methods.

Abstract In this work the kinetics of the $TiCl_4 \rightleftharpoons TiCl_3$ + Cl reaction is studied theoretically. A variable-reaction coordinate transition-state theory (VRC-TST) is used to calculate the high-pressure limit rate coefficients. The interaction energy surface for the VRC-TST step is sampled directly at the CASPT2(6e,4o)/cc-pVDZ level of theory including an approximate treatment of the spin-orbit coupling. The pressure-dependence of the reaction in an argon bath gas is explored using the master equation in conjunction with the optimised VRC-TST transition-state number of states. The collisional energy transfer parameters for the $TiCl_4$–Ar system are estimated via a "one-dimensional minimisation" method and classical trajectories. The Ti–Cl bond dissociation energy is computed using a complete basis set extrapolation technique with cc-pVQZ and cc-pV5Z basis sets. Good quantitative agreement between the estimated rate constants and available literature data is observed. However, the fall-off behaviour of the model results is not seen in the current experimental data. Sensitivity analysis shows that the fall-off effect is insensitive to the choice of model parameters and methods. More experimental work and development of higher-level theoretical methods are needed to further investigate this discrepancy.

Contents

1 Introduction

Titanium tetrachloride, $TiCl_4$, is one of the most commonly used precursors for the industrial synthesis of TiO_2 particles [9]. The main production route involves high-temperature oxidation of $TiCl_4$ in flame reactors, the "chloride" process [7, 16]. TiO_2 particles have wide applications in various fields, with the pigment industry being the largest area.

Despite the importance of the chloride process, knowledge of $TiCl_4$ gas-phase chemistry is still incomplete. This poses difficulties in manipulating the properties of the produced particles (e.g. particle size, surface area) which are critical to its various applications. There have been a number of experimental and computational studies trying to tackle this problem.

Pratsinis et al. [35] investigated the oxidation of $TiCl_4$ vapor in a furnace aerosol reactor between 700–1000 °C. An overall rate constant was derived based on the observation of the $TiCl_4$ conversion. It was observed that the $TiCl_4$ oxidation is first order with respect to $TiCl_4$ and nearly zero order in O_2 up to a 10-fold oxygen excess. Similar observations were made by Kobata et al. [30] and Nakaso et al. [32]. Herzler and Roth [18] examined the thermal decomposition of $TiCl_4$ diluted in argon at 1300–1500 K in a shock tube. The rate coefficients for two successive chlorine abstraction channels ($TiCl_l \rightarrow TiCl_{l-1} + Cl$ for $l = 4, 3$) were calculated *via* measured concentrations of chlorine. The standard enthalpies of formation and bond dissociation energies for $TiCl$, $TiCl_2$ and $TiCl_3$ were measured by Hildenbrand [19] who studied the gaseous equilibria with mass spectrometry.

Several computational studies have been conducted on the Ti–Cl system. Teyssandier and Allendorf [45] estimated the rate coefficients for the unimolecular decomposition of $TiCl_4$, $TiCl_3$ and $TiCl_2$ using RRKM theory at 1000 and 1500 K and a wide range of pressures. Additionally, the Arrhenius parameters for the bimolecular reactions between the titanium chlorides and hydrogen ($TiCl_l$ + H) were estimated *via* Benson's methods and empirical correlation techniques. West et al. [51] calculated the thermochemical properties of a number of important titanium oxychloride species ($Ti_jO_kCl_l$) and proposed the first thermodynamically consistent kinetic mechanism for the oxidation of $TiCl_4$ [52]. This was successfully coupled with a multivariate population balance model [1, 38–40] that solved for the size and structure of each particle. The mechanism was further improved by adding more species and reactions and by computing the rate constants for the important channels [53]. Shirley et al. [41, 42] investigated the role of $AlCl_3$ on the $TiCl_4$ reaction kinetics and extended the detailed thermochemistry of the Ti-containing species proposed by West et al. [51] to include aluminium-titanium-oxychlorides ($Al_iTi_jO_kCl_l$). However, these species were found to have no influence on the gas-phase chemistry. Further work has also been conducted on the adsorption of $TiCl_4$ on the TiO_2 surface, and a new kinetic model for the surface growth was proposed [43].

Although the understanding of the $TiCl_4$ gas-phase chemistry has increased in recent years, there are still areas where our knowledge remains incomplete. In this work we focus on the first and most important reaction in the Ti-Cl system.

$$TiCl_4 \underset{k_{-1}}{\overset{k_1}{\rightleftharpoons}} TiCl_3 + Cl \qquad\qquad\qquad R1$$

Reaction R1 has been previously studied using experimental and computational techniques [18, 45]. However, the experimental investigation was necessarily restricted to a rather narrow range of conditions and the computational study was limited to the use of relatively approximate techniques.

The aim of this paper is to study reaction R1 using a high level of theory and to calculate its rate coefficients for wide range of pressures and temperatures. To achieve this, a variable-reaction-coordinate transition-state theory is combined with multireference quantum chemistry methods to sample the potential energy surface for the reaction. Next, a master equation is constructed and solved for the $TiCl_4$–Ar system using new collision parameters that are calculated as part of work.

2   Theory

2.1   Potential energy surface calculation

In order to explore the current reaction, three different quantum chemistry methods were employed. The starting point was finding the equilibrium geometries and associated frequencies of the reactants and products. This was followed by an accurate prediction of the Ti–Cl bond dissociation energy. Lastly, the long-range interaction potential energy surface was constructed for the $TiCl_3$ + Cl association. The methods are described below.

The geometric structures and vibrational frequencies were obtained *via* unrestricted density functional theory employing the B3LYP functional and the 6-311++G(d,p) basis set [4].

The Ti–Cl bond dissociation energy was calculated from restricted quadratic configuration-interaction calculations with perturbative inclusion of the triplet contribution RQCISD(T) [29], employing the correlation consistent, polarized-valence quadruple and quintuple-ζ basis sets (cc-pVQZ and cc-pV5Z) [8]. The results were then extrapolated to the infinite-basis-set-limit according to the equation [10, 31]

$$E(\infty) = E(l_{\max}) - B/(l_{\max} + 1)^4 \tag{1}$$

where $l_{\max}$ is the maximum angular momentum in the basis set and B is the fitting parameter. The final energy was further updated with the zero-point and spin-orbit corrections. The structure of the fragments and zero-point energies were taken from previous B3LYP calculations. The $(^2P_{1/2} - {}^2P_{3/2})$ splitting of the Cl-atom was taken from experimental measurements [47].

The long-range interaction potential of the $TiCl_3$ + Cl association was obtained using multi-reference second order perturbation theory (CASPT2) [3] employing Dunning's correlation consistent polarized valence double-ζ (cc-pVDZ) basis set [8]. The active space consisted of six electrons in four orbitals (6e,4o). At large separations this corresponds to the radical orbital of $TiCl_3$ and to three equivalent p orbitals of the Cl atom. In order to avoid root flipping problems, the orbitals were optimised in a state-average way for the lowest three singlet states using equal weights. The states correlate with $TiCl_3(1\,^2A'') + Cl(1\,^2P)$ and are degenerate at large separations. Because only one of

these three states is reactive, we chose the one with the lowest energy at each geometry to fit the reactive surface. The structure of the $TiCl_3$ radical was kept fixed at its equilibrium B3LYP/6-311++G(d,p) geometry during this sampling process. The spin-orbit coupling for the $TiCl_3$ + Cl geometries along the minimum energy path was calculated using the wave function constructed as discussed above and the Breit-Pauli Hamiltonian [5].

The B3LYP calculations were performed using Gaussian09 [11]. All other quantum computations were carried out using MOLPRO [50].

2.2 Rate constant calculation

High-pressure. The high pressure-limit rate constant (capture rate) for reaction R1 was calculated using variable-reaction coordinate transition-state theory, VRC-TST [12]. The details of this method have been extensively described elsewhere [12, 26–28]. A brief explanation is provided here.

The reaction rate constant was computed variationally by minimising the reactive flux (proportional to the number of states) with respect to a user defined set of dividing surfaces. The method efficiently incorporates the important couplings and anharmonicities in the nuclear motions by classifying them into conserved and transitional modes [48]. The conserved modes correspond to vibrations of the separated fragments and are assumed to not change along the reaction course. The transitional modes correspond to rotations and translations of the fragments. The number of states for the conserved modes was evaluated quantum mechanically using a direct counting algorithm [6, 44]. The transitional modes were treated with phase space integrals [27] evaluated via Monte Carlo integration thus incorporating fully anharmonic and mode-coupled transitional mode contribution to the transition-state partition function

The VRC-TST transition-state dividing surfaces were determined by pivot points associated with each fragment. These points were used as centers of rotation and to define the distance between the fragments. The transition-state number of states were then minimised with respect to both the position and relative separation of the pivot points.

In this work, the final computation of the available number of states was performed at the energy, E, and angular momentum, J, resolved (microcanonical) level. The transition-state dividing surfaces were constructed by placing one pivot point on the center of mass of the $TiCl_3$ fragment and one pivot point on the chlorine atom. The separation distances were varied on a grid from 5.5 to 18 au. A grid spacing of 0.2-0.3 was used for small (5.5-10 au) separations and 0.5 au for large (10-18 au) separations.

The overall expression for the high-pressure recombination rate coefficient at temperature T is given as [49]

$$k(T) = \gamma \frac{1}{2\pi} g_e \frac{\sigma_1 \sigma_2}{\sigma^{\ddagger}} \left(\frac{2\pi}{\mu k_B T} \right)^{3/2} \frac{\int dE dJ N^{\ddagger}(E,J) e^{-E/k_B T}}{Q_1(T) Q_2(T)} \tag{2}$$

where g_e is the electronic degeneracy factor, σ_1, σ_2 and $\sigma^{\dagger}$ are the rotational symmetry numbers for the reactants and transition state, μ, Q_1 and Q_2 are the reduced mass and partition functions of the reactants, respectively. The quantity $N^{\ddagger}(E,J)$ is the transition-

state number of states at the E, J-resolved level. Additionally, a correction factor γ equal to 0.9 was used to account for recrossing as suggested in the literature [17] for atom-molecule reactions.

The spin-orbit coupling effect was not directly included in the interaction potential. Instead an approximation suggested by Jasper et al. [24] was used to correct the final results. The correction is given as,

$$k^{\text{so}}(T) = k(T) \exp\left(-\frac{C(T)E_{\text{so}}}{RT}\right) \tag{3}$$

where k^{so} and $k(T)$ are the rate constants with and without spin-orbit coupling included and the E_{so} is an asymptotic value of the spin-orbit stabilisation energy (in this case $E_{\text{so}} = 0.78$ kcal mol^{-1} at the given level of theory). The coefficient, C, depends on the temperature and can be estimated using the following equation,

$$C(T) = 1 - \frac{\varepsilon(\text{CVT}^*(T))}{E_{\text{so}}} \tag{4}$$

where $\varepsilon(\text{CVT}^*(T))$ is the value of spin-orbit stabilisation energy at the optimal dividing surface for a given temperature.

A priori pressure dependence. The pressure dependence was calculated using a chemical master equation [13, 28] and the exponential down model [46].

The collisional parameters were calculated using a full-dimensional TiCl$_4$ + Ar potential energy surface based on the separable pairwise approximation [22]. The intramolecular TiCl$_4$ potential energy surface was modeled using a slightly modified UFF parametrization [37], where the atomic radii of Ti and Cl were decreased by 5% to improve the equilibrium Ti-Cl bond distance in TiCl$_4$ from 2.33 to 2.22 Å (in better agreement with the experimental value [33] of 2.17 Å). This adjustment improved the rotational constant to 0.036 cm^{-1}, in good agreement with the experimental value of 0.038 cm^{-1}. The harmonic vibrational frequencies calculated using the modified UFF parametrization were 143, 160, 354, and 511 cm^{-1}, which are in fair agreement with the experimental values of 114, 136, 389, and 498 cm^{-1}. Although this description of the TiCl$_4$ potential energy surface is approximate, collisional parameters have been shown to be fairly insensitive to the details of the intramolecular potential of the unimolecular reactant [21, 46], and we do not expect deficiencies in the intramolecular TiCl$_4$ potential to be a significant source of uncertainty in the collision parameters calculated below.

The intermolecular potential for TiCl$_4$ + Ar was modeled using separable pairwise Buckingham interactions parameterized to reproduce the results of counterpoise corrected CCSD(T)/CBS calculations. This representation of the intermolecular potential has been shown to accurately reproduce the repulsive wall energies for systems involving atomic baths, which are important for predicting accurate collision parameters [22].

Next, Lennard-Jones collision parameters were calculated using the "one dimensional minimization" method [23] and the potential energy surface described above. This scheme has been shown to accurately predict collision rates (within 15% of experimentally inferred values) for a wide variety of systems [23].

Table 1: *Stationary point energies for reaction R1.*

Species	B3LYP[a] 6-311++G(d,p)	RQCISD(T)[a] VTZ	VQZ	V5Z	CBS[b]
		E_0 (hartree)			
$TiCl_4$	-2690.651	-2687.786	-2687.887	-2687.921	-2687.953
$TiCl_3$	-2230.350	-2227.976	-2228.053	-2228.080	-2228.104
Cl	-460.167	-459.672	-459.693	-459.700	-459.706
		D_0 (kcal mol^{-1})[c]			
$TiCl_3 + Cl$	81.762	84.733	85.981	86.996	87.942

[a] Electronic B3LYP and RQCISD(T) energies.

[b] Energies extrapolated with Eq. 1 using cc-pVQZ and cc-pV5Z basis sets.

[c] Zero point and spin orbit corrections included throughout.

Finally, the range parameter, α, of the exponential down model was calculated using classical trajectories. The exponential down model estimates the probability of a given amount of energy being transferred in a collision between species. The model assumes that the probability to transfer energy in a single collision event depends exponentially on the amount of energy that is transferred. Small amounts of energy are more likely to be transferred than large amounts of energy. According to this model the probability is given as:

$$P(E, E') = \frac{1}{N(E')} \exp\left(-\frac{E - E'}{\alpha}\right) \quad E \geq E' \tag{5}$$

where, $P(E, E')$ is the probability of the process where a reactant molecule, with initial energy E' undergoes a collision with a bath gas and ends up with internal energy E. $N(E')$ is the normalisation constant and α is the range parameter.

When reasonable conditions are met, α can be shown to be equal to the average energy in deactivating collisions, $\langle \Delta E_d \rangle$ [13]. The probability for the upward collisions can then be found via the microscopic reversibility law. Values of $\langle \Delta E_d \rangle$ at various temperatures suitable for use in kinetic models can be straightforwardly calculated using ensembles of highly-vibrationally excited trajectories, as described in detail elsewhere [25]. Here, $\langle \Delta E_d \rangle$ was calculated at 1000 and 2000 K using the potential energy surface described above and ensembles of 1200 trajectories. These values were then fitted using the following functional form,

$$\langle \Delta E_d \rangle = \langle \Delta E_d^0 \rangle (T/300\text{K})^n \tag{6}$$

where, T is a tempreature and $\langle \Delta E_d^0 \rangle$ and n are the pre-factor and exponent to be fitted. This function was eventually used to model collisional energy transfer in the master equation calculations.
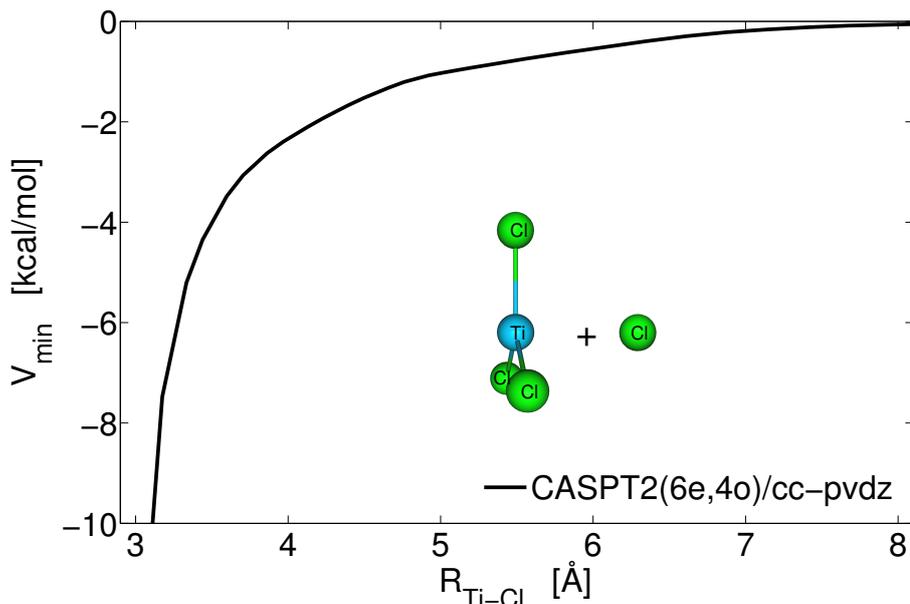
Figure 1: *Interaction energy between TiCl₃ and Cl along the minimum VRC-TST energy path (see text). The structure of the TiCl₃ fragment was kept frozen at its UB3LYP equilibrium geometry during the sampling process.*

3 Results and discussion

3.1 Electronic structure calculations

The stationary point energies for reaction R1 are summarised at different levels of theory in **Table 1**. Additionally, the Ti–Cl bond dissociation energies, D_0, are provided. It can be seen that D_0 increases with the size of the basis set. The final, recommended value of D_0 is 87.94 kcal mol^{-1} and was estimated via the complete basis set extrapolation technique. This compares well with the Allendorf et al. [2] data where apart from the experiments they also performed coupled-cluster [36] calculations combined with a bond-additivity correction and found that D_0 lies in the range 86.5–91.7 kcal mol^{-1}.

To the best of our knowledge, the only experimental data that exist for the D_0 parameter are the high-temperature flow reactor (HTFR) measurements of Allendorf et al. [2] ($D_0 \geq 98$ kcal mol^{-1}) and the Hildenbrand's [19] mass-spectrometric measurements (D_0 = 92.8 kcal mol^{-1}) .

The Allendorf et al. [2] data were obtained by using the Gorin Model combined with the master equation to adjust the bond dissociation energy so that their theoretical predictions match experimental observations. Noting that both the experiments and these theoretical calculations each have associated error bars of a factor of 2-3, it is considered that the bond dissociation energy derived by the Allendorf et al. [2] is rather too high. Allendorf et al. [2] themselves stated that the found D_0 is surprisingly higher than any previous estimates of this parameter and suggested further theoretical or experimental work.

The Hildenbrand's [19] experimental data, were obtained by monitoring the reaction equi-
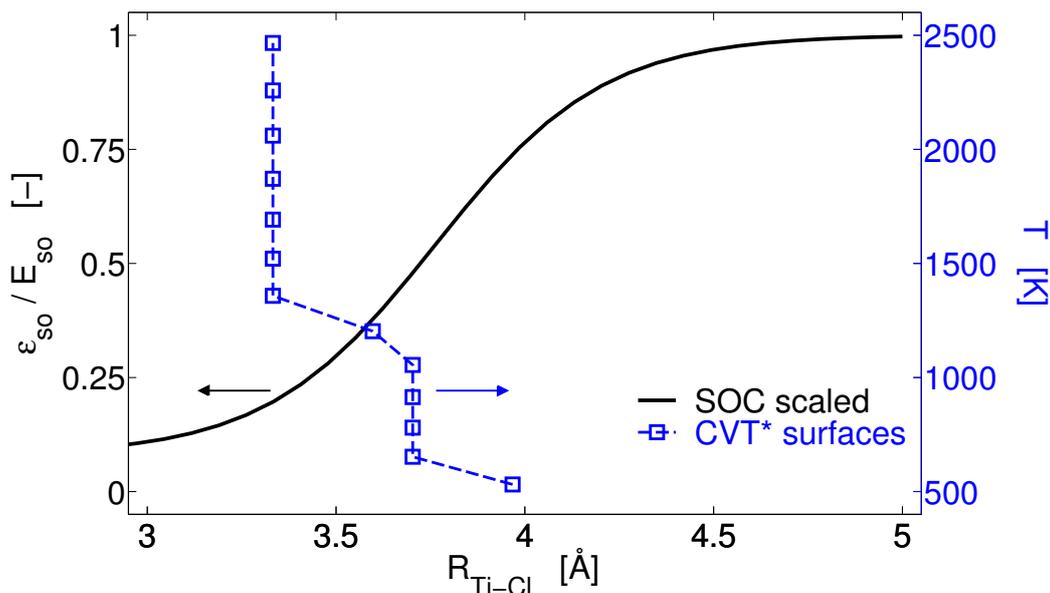
Figure 2: *Spin-orbit coupling energy, ε_{so}, scaled by its asymptotic value, E_{so} (0.78 kcal mol^{-1}), along the minimum-energy path. The dashed line with square markers shows location of the optimal CVT* dividing surfaces as a function of the temperature (right axis).*

libria of the Ti-Cl species with AgCl by effusion beam mass spectrometry at various temperatures. The required thermochemical properties of the Ti-Cl species were then evaluated from third-law analysis of the derived equilibrium data while relying on the accurately known dissociation energy of the AgCl species. In this procedure, however, the low-lying electronic states of the Ti-Cl species were not taken into account which are important in achieving accurate predictions. This can explain observed 4.9 kcal mol^{-1} difference between ours and initial Hildenbrand's [19] results. In a later work, Hildenbrand [20] updated his experimental data with an energetic effect caused by these low-lying electronic states and provided the revised thermochemistry for the Ti-Cl species. After this correction, the reported value of the bond dissociation energy was equal to 89.9 kcal mol^{-1} at 298 K. If our bond dissociation energy is brought to the same temperature then it equals 88.6 kcal mol^{-1} at 298 K. This is only 1.3 kcal mol^{-1} lower than the revised Hildenbrand's [20] predictions and is well within his experimental uncertainties which are estimated to be within ±2 kcal mol^{-1}.

Given a good agreement with the literature data, especially with the revised Hildenbrand's [20] results which are the most detailed among currently available estimates, it is believed that our CBS/RQCISD(T) predictions are enough accurate and provide an important theoretical complement for the studied reaction.

In order to estimate the spin-orbit coupling correction (SOC) via equations 3 and 4, the reactive flux was optimised at the canonical (thermally-resolved) level. This technique has the advantage of simplifying the analysis of the reaction kinetics, where one optimal dividing surface is assigned to each temperature. However, it is less accurate than the microcanonical computations and it was only used to estimate the SOC term.
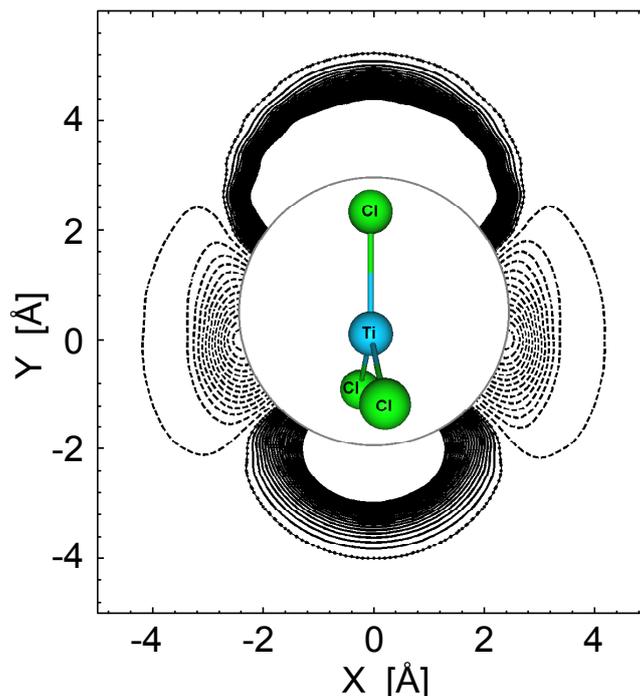
Figure 3: *Contour plot of the CASPT2(6e,4o)/cc-pVDZ interaction potential for the TiCl$_3$ + Cl association. The plotting plane is spanned by a vector pointing from the Ti atom towards bonded the upper chlorine atom and by a C$_3$ symmetry axis. The solid and dashed contours represent repulsive and attractive energies respectively. A zero energy contour is shown by the solid line with dot markers. The energy increment is 1 kcal/mol. The circle in the middle of the plot covers an irrelevant unplotted region of the potential surface.*

Figure 1 shows the minimum VRC-TST interaction energy found in the sampling process. The reported energies at each considered fragments' separation, measured as a distance between Ti atom in TiCl$_3$ and approaching Cl atom ($R_{\text{Ti-Cl}}$), were obtained by performing a large number of single point calculations at different Cl approach angles. The number of samples taken at each Ti–Cl distance varied from 200 to 2000 depending on the convergence of the random sampling algorithm. The geometry of the TiCl$_3$ was kept frozen at its UB3LYP equilibrium geometry during this process. The corresponding values of the scaled spin-orbit coupling stabilisation energies (SOC) are shown on **Figure 2**. It can be seen that the SOC strongly depends on the Ti-Cl distance. It is negligible for small separations ($R_{\text{Ti-Cl}} < 3$ Å) and it reaches its asymptotic value of 0.78 kcal mol^{-1} at about 4.5 Å. The optimal canonical surfaces (CVT*) are depicted on Figure 2 as a dashed line with square markers (right-hand axis). These are the locations of the bottleneck giving the minimal rate constant at each temperature. It can be seen that the kinetically relevant separations at this level of theory are lying at 3.3-4 Å. In this region, the spin-orbit coupling is within 20-75% of its maximum value.

Figure 3 shows part of the potential energy surface computed at the CASPT2 level of theory. The plotting plane includes a C$_3$ symmetry axis of the TiCl$_3$ radical and one of the Ti-Cl bonds. Two chlorine addition sites are identified. These are the areas where the
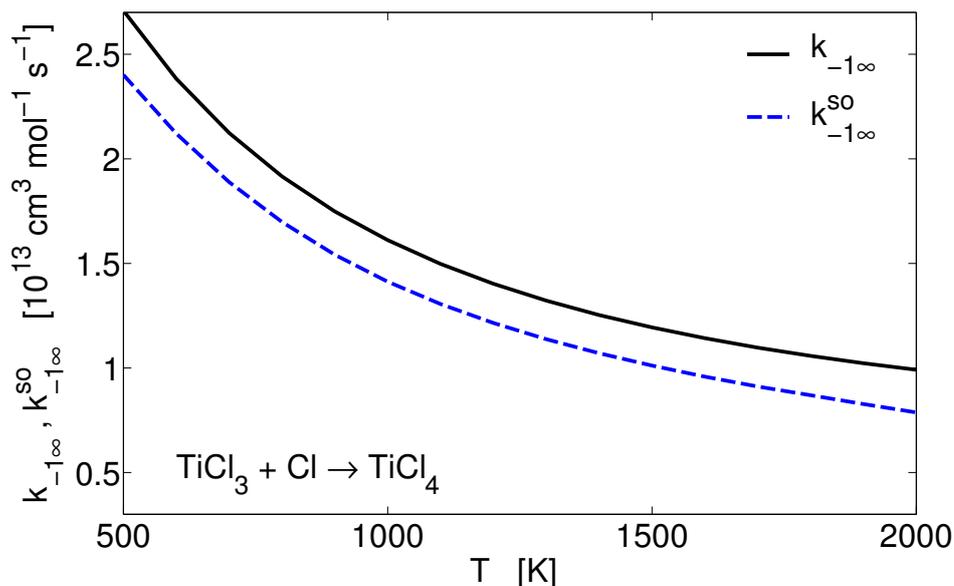
Figure 4: *High-pressure association rate constants, $k_{-1\infty}$ and $k^{so}_{-1\infty}$ as a function of the temperature. The dashed and solid lines represent rates with and without spin-orbit correction, respectively.*
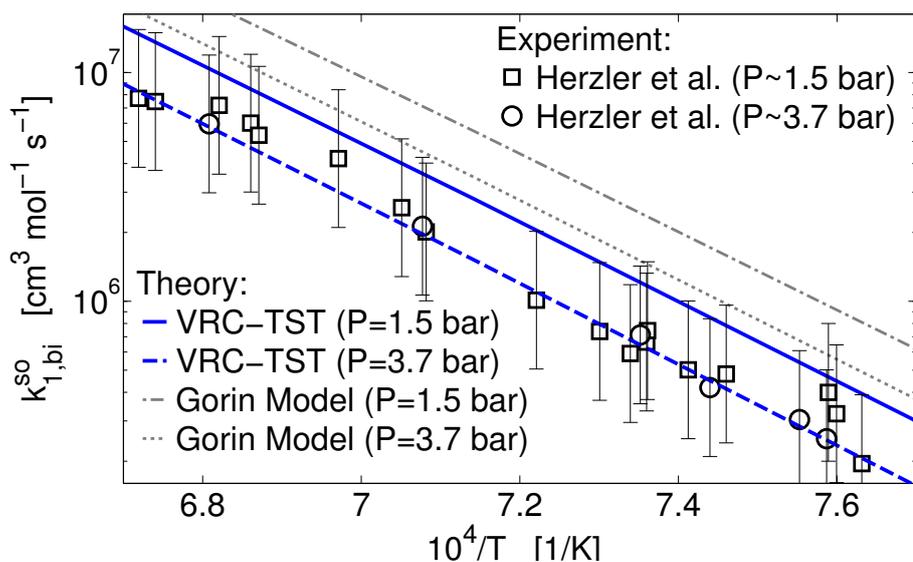
Figure 5: *Arrhenius plot of the calculated k^{so}_1 rate coefficient at P=1.5 and 3.7 bar versus experimental data.*

potential is strongly attractive (negative). The total rate constant is the sum of the chlorine additions from both sites and, because of the symmetry, was computed by evaluating the reactive flux through one site and multiplying it by a factor of two.
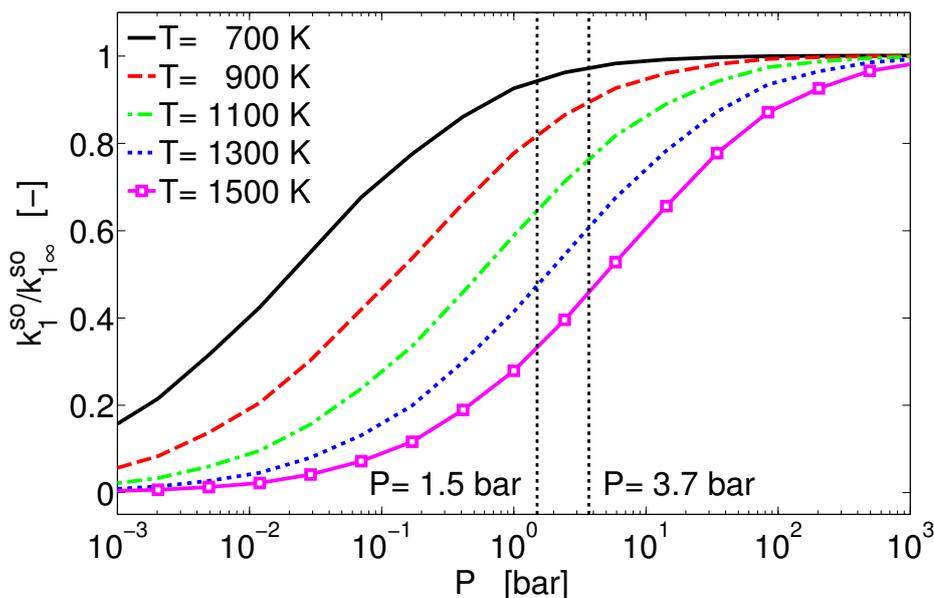
Figure 6: *Rate coefficients in the dissociation direction as a function of pressure at selected temperatures. The rates are normalised by their high-pressure limit values.*

3.2 Rate constants

The computed high-pressure limited association rate constant is depicted on **Figure 4** with and without spin-orbit correction. The spin-orbit correction reduces the final rate coefficient by 10-15%. This is consistent with the literature [24], where a typical change caused by this effect was found to be within 10-13% for analogous kinetic systems.

A negative temperature dependence can be observed, which is common for barrier-less reactions. This occurs when an increase in temperature shifts the transition state along the barrier-less potential towards smaller separations (see Fig. 2). This shift causes strong steric repulsion between the reactants while they try to form an energetically favourable configuration for the reaction to take place. Because of this, only a fraction of these configurations are reactive while the others are strongly repulsive, giving rise to an inverse temperature dependence.

Figure 5 shows the calculated bimolecular rate constant $k_{1,\mathrm{bi}}^{\mathrm{so}}$ at two different pressures versus the experimental data of Herzler and Roth [18]. The bimolecular rate constant was obtained from the predicted first order rate coefficient k_1^{so} by adding the concentration of the bath gas at the corresponding pressure. The error bars represent the uncertainty in the experimental measurements implied by Herzler et al. (about a factor of two). It can be seen that the results from VRC-TST and ME computations are within the experimental error bars. However, the fall-off behaviour evident in the computed rate constants is not seen in the experimental observations, where the rates are about the same at the two pressures considered.

The cause of the observed discrepancy is unclear. A number of sensitivity studies were performed to test how the fall-effect is influenced by the model parameters. In particular,

12

Table 2: *Predicted rate constants for reaction R1 at different temperatures in modified Arrhenius and Troe form. The master equation parameters used in the pressure-dependency computations are also reported.[a]*

Reaction		$TiCl_4 \underset{k_{-1}}{\overset{k_1}{\rightleftharpoons}} TiCl_3 + Cl$		
		500 - 2500 K (Arrhenius form)[b]		
	P	A	n	E_0
$k^{so}_{-1\infty}$	inf	6.607×10^{14}	-0.583	-141.4
	0.001	4.801×10^{46}	-10.805	47960
	0.01	2.210×10^{46}	-9.805	48539
k^{so}_1	0.1	2.491×10^{44}	-8.970	48810
	1	1.054×10^{40}	-7.477	48414
	10	3.344×10^{33}	-5.434	47274
	100	1.119×10^{27}	-3.468	45888
		500 - 2500 K (Troe form)[c]		
$k^{so}_{1\infty}$	inf	5.322×10^{21}	-1.883	44631
k^{so}_{1o}	lowP	1.645×10^{52}	-9.42	45968
		$a = 0.777, T^{***} = 31, T^* = 804, T^{**} = 3581$		

Master Equation Parameters for $TiCl_4$–Ar system.[d]

$\langle \Delta E_d^0 \rangle = 1000 \text{ cm}^{-1}$ [e]

$\sigma = 4.507 \text{ Å} \quad \varepsilon = 259.050 \text{ cm}^{-1}$

---

[a] Units are bars, cm^3, seconds, kelvins and moles.

[b] Arrhenius equation of the form: $k = AT^n \exp(-E_0/T)$.

[c] Troe equation as in ref. [14] for P=$10^{-10} - 10^5$ bar.

[d] This work, see text.

[e] Pre-factor in exponent down model of the form:
$\langle \Delta E_d \rangle = \langle \Delta E_d^0 \rangle (T/300 K)^{0.5}$.

the pre-factor in the exponential down model and the Lennard-Jones constants were varied by ±50% which is well beyond the uncertainties of the methods used to obtain these parameters. However, no reduction in the fall-off behaviour was observed.

A further sensitivity analysis was conducted to check the sensitivity to any errors in the potential energy surface. In order to do that a Gorin Model [34] implemented in the Unimol code [15] was employed to recompute the rate constants. This technique eliminates the complexity of the VRC-TST method by replacing the multidimensional potential by a simple one dimensional potential. All the remaining model parameters were the same as in the previous calculations. Figure 5 shows the outcomes of these computations. It can be seen that again no significant reduction in the fall-off effect was obtained.

It is worth noting that Teyssandier and Allendorf [45] studied reaction R1 using the Gorin Model with molecular hydrogen as a bath gas. They provided the final rates as a function of pressure and temperature in Troe form [14]. No fall-off effect can be observed in the Troe rates for the range of experimental conditions considered by Herzler and Roth [18]. We repeated the Gorin Model calculations using exactly the same methods and parameters as Teyssandier and Allendorf [45]. A fall-off effect of the same magnitude as in our Gorin computations with argon was observed in the raw reaction rates. However, this behaviour was lost once the data were fitted in Troe form.

In summary, given all the outcomes gathered so far, it was decided to present our VRC-TST and ME results as they are. The cause of the discrepancy between the calculated and measured fall-off remains an open question. Both the theory and experiment have similarly-sized error bars of a factor of 2, and agree within this level of uncertainty. Smaller error bars would be required to discriminate any sub-factor-of-2 features, including the details of the fall-off behaviour. If possible, experimental measurements of the high pressure limit of the reaction would provide further valuable insight. This information would help to test the accuracy of the employed methods in the case where the complex collision-induced transitions do not influence the reaction rate.

Figure 6 depicts the normalised rate constant k_1^{so}. It can be seen that for the experimentally studied conditions (P=1.5–3.7 bar and T=1200–1500 K) this rate is within 30–70% of its high-pressure limit value. It is a typical fall-off regime. The computed reaction rates were fitted to the modified Arrhenius equation for the selected conditions and additionally to the Troe formula [14] for the full range of pressures and temperatures considered in this work. The fitted rate parameters are given in **Table 2** along with the Lennard Jones coefficients and pre-factor $\langle \Delta E_d^0 \rangle$ for the exponential down model. The maximum fitting errors are within a factor of 1.1 and 2 for the Arrhenius and Troe formulas respectively.

4   Conclusions

A theoretical study of the kinetics of the $TiCl_4 \rightleftharpoons TiCl_3 + Cl$ reaction has been performed for a wide range of temperatures and pressures. The high-pressure limit rate coefficients in the association direction have been calculated via variable-reaction coordinate transition state theory combined with multireference CASPT2(6e,4o)/cc-pVDZ electronic structure calculations. Additionally, an approximate treatment of the spin-orbit coupling effect has been introduced resulting in a 10-15% reduction in the final rates.

The pressure dependence of the reaction has been calculated by constructing and solving the master equation using the number of states for the optimised transition state from the VRC-TST step. This is the first study that has estimated this effect in reaction R1 without making any assumptions about the values of the master equation collision parameters. Instead, they have been computed from first-principles using "one dimensional minimisation" and classical trajectories methods.

The calculated rate coefficients are in a good quantitative agreement with the available literature data. However, the low pressure fall-off behaviour visible from the modelling outcomes is in contrast with experimental observations. In order to investigate this dis-

crepancy a number of sensitivity studies has been performed with respect to the model parameters and the methods employed. No significant change was observed in the predicted low-pressure fall-off behaviour and the cause of the discrepancy still remains unclear. The development of higher-level methods in addition to experimental measurements at the high-pressure limit of this reaction would be helpful in resolving this puzzle.

Acknowledgements

References

[1] J. Akroyd, A. Smith, R. Shirley, L. R. McGlashan, and M. Kraft. A coupled CFD-population balance approach for nanoparticle synthesis in turbulent reacting flows. *Chem. Eng. Sci.*, 66(17):3792–3805, 2011. doi:10.1016/j.ces.2011.05.006.

[2] M. D. Allendorf, C. L. Janssen, M. E. Colvin, C. F. Melius, I. M. B. Nielsen, T. H. Osterheld, and P. Ho. Thermochemistry of gas-phase species relevant to titanium nitride CVD. In M. Meyyappan, D. J. Economou, and S. W. Butler, editors, *Proceedings of the Symposium on Process Control, Diagnostics, and Modeling in Semiconductor Manufacturing I*, chapter 95-2, pages 393–399. The Electrochemical Society, Pennington, NJ, 1995.

[3] K. Andersson, P.-Å. Malmqvist, and B. O. Roos. Second-order perturbation theory with a complete active space self–consistent field reference function. *J. Chem. Phys.*, 96(2):1218–1226, 1992. doi:10.1063/1.462209.

[4] A. D. Becke. Density-functional thermochemistry. III. The role of exact exchange. *J. Chem. Phys.*, 98(7):5648–5651, 1993. doi:10.1063/1.464913.

[5] A. Berning, M. Schweizer, H.-J. Werner, P. J. Knowles, and P. Palmieri. Spin-orbit matrix elements for internally contracted multireference configuration interaction wavefunctions. *Mol. Phys.*, 98(21):1823–1833, 2010. doi:10.1080/00268970009483386.

[6] T. Beyer and D. F. Swinehart. Algorithm 448: Number of multiply-restricted partitions. *Comm. ACM*, 16(6):379–379, 1973. doi:10.1145/362248.362275.

[7] J. C. Deberry, M. Robinson, M. D. Pomponi, A. J. Beach, Y. Xiong, and K. Akhtar. Controlled vapor phase oxidation of titanium tetrachloride to manufacture titanium dioxide, May 14 2002. US Patent 6,387,347, url: http://www.google.com/patents/US6387347.

[8] T. H. Dunning. Gaussian basis sets for use in correlated molecular calculations. I. The atoms boron through neon and hydrogen. *J. Chem. Phys.*, 90(2):1007–1023, 1989. doi:10.1063/1.456153.

[9] J. Emsley. *Molecules at an Exhibition*. Oxford University Press, 1999.

[10] D. Feller and D. A. Dixon. Extended benchmark studies of coupled cluster theory through triple excitations. *J. Chem. Phys.*, 115(8):3484–3496, 2001. doi:10.1063/1.1388045.

[11] M. J. Frisch, G. W. Trucks, H. B. Schlegel, G. E. Scuseria, M. A. Robb, J. R. Cheeseman, G. Scalmani, V. Barone, B. Mennucci, G. A. Petersson, H. Nakatsuji, M. Caricato, X. Li, H. P. Hratchian, A. F. Izmaylov, J. Bloino, G. Zheng, J. L. Sonnenberg, M. Hada, M. Ehara, K. Toyota, R. Fukuda, J. Hasegawa, M. Ishida, T. Nakajima, Y. Honda, O. Kitao, H. Nakai, T. Vreven, J. A. Montgomery, Jr., J. E. Peralta,

F. Ogliaro, M. Bearpark, J. J. Heyd, E. Brothers, K. N. Kudin, V. N. Staroverov, R. Kobayashi, J. Normand, K. Raghavachari, A. Rendell, J. C. Burant, S. S. Iyengar, J. Tomasi, M. Cossi, N. Rega, J. M. Millam, M. Klene, J. E. Knox, J. B. Cross, V. Bakken, C. Adamo, J. Jaramillo, R. Gomperts, R. E. Stratmann, O. Yazyev, A. J. Austin, R. Cammi, C. Pomelli, J. W. Ochterski, R. L. Martin, K. Morokuma, V. G. Zakrzewski, G. A. Voth, P. Salvador, J. J. Dannenberg, S. Dapprich, A. D. Daniels, Ö. Farkas, J. B. Foresman, J. V. Ortiz, J. Cioslowski, and D. J. Fox. Gaussian09 Revision E.01, 2009. Gaussian Inc. Wallingford CT 2009.

[12] Y. Georgievskii and S. J. Klippenstein. Variable reaction coordinate transition state theory: Analytic results and application to the $C_2H_3 + H \rightarrow C_2H_4$ reaction. *J. Phys. Chem. A*, 118(12):5442–5455, 2003. doi:10.1063/1.1539035.

[13] Y. Georgievskii, J. A. Miller, M. P. Burke, and S. J. Klippenstein. Reformulation and solution of the master equation for multiple-well chemical reactions. *J. Phys. Chem. A*, 117(46):12146–12154, 2013. doi:10.1021/jp4060704.

[14] R. G. Gilbert, K. Luther, and J. Troe. Theory of thermal unimolecular reactions in the fall-off range. II. weak collision rate constants. *Ber. Bunsenges. Phys. Chem.*, 87 (2):169–177, 1983. doi:10.1002/bbpc.19830870218.

[15] R. G. Gilbert, S. C. Smith, and M. J. T. Jordan. UNIMOL program suite, 1993.

[16] R. A. Gonzalez, C. D. Musick, and J. N. Tilton. Process for controlling agglomeration in the manufacture of TiO_2, Apr. 16 1996. US Patent 5,508,015, url: http://www.google.com/patents/US5508015.

[17] L. B. Harding, Y. Georgievskii, and S. J. Klippenstein. Predictive theory for hydrogen atom-hydrocarbon radical association kinetics. *J. Phys. Chem. A*, 109(21): 4646–4656, 2005. doi:10.1021/jp0508608.

[18] J. Herzler and P. Roth. High-temperature decomposition of $TiCl_4$ based on Cl-concentration measurements. *Proc. Comb. Inst.*, 29(1):1353–1359, 2002. doi:10.1016/S1540-7489(02)80166-3.

[19] D. L. Hildenbrand. Thermochemical properties of gaseous TiCl, $TiCl_2$, and $TiCl_3$. *High. Temp. Mat. Sci.*, 35(2):151–158, 1996.

[20] D. L. Hildenbrand. Low-lying electronic states and revised thermochemistry of TiCl, $TiCl_2$, and $TiCl_3$. *J. Phys. Chem. A*, 113(8):1472–1474, 2009. doi:10.1021/jp807913c.

[21] X. Hu and W. L. Hase. Effect of anharmonicity on intermolecular energy transfer from highly vibrationally excited molecules. *J. Phys. Chem.*, 92(14):4040–4046, 1988. doi:10.1021/j100325a011.

[22] A. W. Jasper and J. A. Miller. Theoretical unimolecular kinetics for $CH_4 + M \leftrightarrow CH_3 + H + M$ in eight baths, M = He, Ne, Ar, Kr, H_2, N_2, CO, and CH_4. *J. Phys. Chem. A*, 115(24):6438–6455, 2011. doi:10.1021/jp200048n.

[23] A. W. Jasper and J. A. Miller. Lennard-Jones parameters for combustion and chemical kinetics modeling from full-dimensional intermolecular potentials. *Combust. Flame*, 161(1):101–110, 2014. doi:10.1016/j.combustflame.2013.08.004.

[24] A. W. Jasper, S. J. Klippenstein, and L. B. Harding. The effect of spin-orbit splitting on the association kinetics of barrierless halogen atom-hydrocarbon radical reactions. *J. Chem. Phys.*, 114(18):5759–5768, 2010. doi:10.1021/jp1015092.

[25] A. W. Jasper, M. C. Oana, and J. A. Miller. "Third-body" collision efficiencies for combustion modeling: Hydrocarbons in atomic and diatomic baths. *Proc. Comb. Inst.*, 35(1):197–204, 2015. doi:10.1016/j.proci.2014.05.105.

[26] S. J. Klippenstein. A bond length reaction coordinate for unimolecular reactions. II. Microcanonical and canonical implementations with application to the dissociation of NCNO. *J. Chem. Phys.*, 94(10):6469–6482, 1991. doi:10.1063/1.460276.

[27] S. J. Klippenstein. An efficient procedure for evaluating the number of available states within a variably defined reaction coordinate framework. *J. Phys. Chem.*, 98 (44):11459–11464, 1994. doi:10.1021/j100095a032.

[28] S. J. Klippenstein, Y. Georgievskii, and L. B. Harding. Predictive theory for the combination kinetics of two alkyl radicals. *PCCP*, 8:1133–1147, 2006. doi:10.1039/B515914H.

[29] P. J. Knowles, C. Hampel, and H.-J. Werner. Coupled cluster theory for high spin, open shell reference wave functions. *J. Chem. Phys.*, 99:5219–5227, 1993. doi:10.1063/1.465990.

[30] A. Kobata, K. Kusakabe, and S. Morooka. Growth and transformation of TiO_2 crystallites in aerosol reactor. *AIChE J.*, 37(3):347–359, 1991. doi:10.1002/aic.690370305.

[31] J. M. L. Martin. Ab initio total atomization energies of small molecules - towards the basis set limit. *Chem. Phys. Lett.*, 259(5–6):669–678, 1996. doi:10.1016/0009-2614(96)00898-6.

[32] K. Nakaso, K. Okuyama, M. Shimada, and S. Pratsinis. Effect of reaction temperature on CVD-made TiO_2 primary particle diameter. *Chem. Eng. Sci.*, 58(15): 3327–3335, 2003. doi:10.1016/S0009-2509(03)00213-6.

[33] NIST Computational Chemistry Comparison and Benchmark Database, 2015. NIST Standard Reference Database Number 101. Release 17b, September 2015, Editor: Russell D. Johnson III. url: http://cccbdb.nist.gov.

[34] I. G. Pitt, R. G. Gilbert, and K. R. Ryan. Extended Gorin Model for radical-radical recombination reactions. *J. Phys. Chem.*, 99:239–247, 1995. doi:10.1021/j100001a037.

[35] S. E. Pratsinis, B. Hebi, B. Pratim, M. Frenklach, and S. V. R. Mastrangelo. Kinetics of titanium(IV) chloride oxidation. *J. Am. Ceram. Soc.*, 73(7):2158–2162, 1990. doi:10.1111/j.1151-2916.1990.tb05295.x.

[36] K. Raghavachari, G. W. Trucks, J. A. Pople, and M. Head-Gordon. A fifth-order perturbation comparison of electron correlation theories. *Chem. Phys. Lett.*, 157(6): 479–483, 1989. doi:10.1016/S0009-2614(89)87395-6.

[37] A. K. Rappé, C. J. Casewit, K. S. Colwell, W. A. Goddard, and W. M. Skiff. UFF, a full periodic table force field for molecular mechanics and molecular dynamics simulations. *J. Am. Chem. Soc.*, 114(25):10024–10035, 1992. doi:10.1021/ja00051a040.

[38] M. Sander, R. H. West, M. S. Celnik, and M. Kraft. A detailed model for the sintering of polydispersed nanoparticle agglomerates. *Aerosol Sci. Tech.*, 43(10):978–989, 2009. doi:10.1080/02786820903092416.

[39] S. Shekar, W. J. Menz, A. J. Smith, M. Kraft, and W. Wagner. On a multivariate population balance model to describe the structure and composition of silica nanoparticles. *Comput. Chem. Eng.*, 43(10):130–147, 2012. doi:10.1016/j.compchemeng.2012.04.010.

[40] S. Shekar, A. J. Smith, W. J. Menz, M. Sander, and M. Kraft. A multidimensional population balance model to describe the aerosol synthesis of silica nanoparticles. *J. Aerosol Sci.*, 44:83–98, 2012. doi:10.1016/j.jaerosci.2011.09.004.

[41] R. Shirley, Y. Liu, T. Totton, R. H. West, and M. Kraft. First-principles thermochemistry for the combustion of a $TiCl_4$ and $AlCl_3$ mixture. *J. Phys. Chem. A*, 113(49): 13790–13796, 2009. doi:10.1021/jp905244w.

[42] R. Shirley, W. Phadungsukanan, M. Kraft, J. Downing, N. E. Day, and P. Murray-Rust. First-principles thermochemistry for gas phase species in an industrial rutile chlorinator. *J. Phys. Chem. A*, 114(43):11825–11832, 2010. doi:10.1021/jp106795p.

[43] R. Shirley, J. Akroyd, L. A. Miller, O. R. Inderwildi, U. Riedel, and M. Kraft. Theoretical insights into the surface growth of rutile TiO_2. *Combust. Flame*, 158(10): 1868–1876, 2011. doi:10.1016/j.combustflame.2011.06.007.

[44] S. E. Stein and B. S. Rabinovitch. Accurate evaluation of internal energy level sums and densities including anharmonic oscillators and hindered rotors. *J. Chem. Phys.*, 58(6):2438–2445, 1973. doi:10.1063/1.1679522.

[45] F. Teyssandier and M. D. Allendorf. Thermodynamics and kinetics of gas-phase teactions in the Ti-Cl-H system. *J. Electrochem. Soc.*, 145(6):2167–2178, 1998. doi:10.1149/1.1838613.

[46] J. Troe. Theory of thermal unimolecular reactions at low pressures. i. solutions of the master equation. *J. Chem. Phys.*, 66(11):4745–4757, 1977. doi:10.1063/1.433837.

[47] H. Uehara and K. Horiai. Infrared-microwave double resonance of atomic chlorine on laser-magnetic-resonance fine-structure transitions. *J. Opt. Soc. Am. B*, 4(7): 1217–1221, 1987. doi:10.1364/JOSAB.4.001217.

[48] D. M. Wardlaw and R. A. Marcus. RRKM reaction rate theory for transition states of any looseness. *Chem. Phys. Lett.*, 110(3):230–234, 1984. doi:10.1016/0009-2614(84)85219-7.

[49] D. M. Wardlaw and R. A. Marcus. Unimolecular reaction rate theory for transition states of any looseness. 3. Application to methyl radical recombination. *J. Phys. Chem.*, 90(21):5383–5393, 1986. doi:10.1021/j100412a098.

[50] H.-J. Werner, P. J. Knowles, G. Knizia, F. R. Manby, M. Schütz, P. Celani, W. Györffy, D. Kats, T. Korona, R. Lindh, A. Mitrushenkov, G. Rauhut, K. R. Shamasundar, T. B. Adler, R. D. Amos, A. Bernhardsson, A. Berning, D. L. Cooper, M. J. O. Deegan, A. J. Dobbyn, F. Eckert, E. Goll, C. Hampel, A. Hesselmann, G. Hetzer, T. Hrenar, G. Jansen, C. Köppl, Y. Liu, A. W. Lloyd, R. A. Mata, A. J. May, S. J. McNicholas, W. Meyer, M. E. Mura, A. Nicklass, D. P. O'Neill, P. Palmieri, D. Peng, K. Pflüger, R. Pitzer, M. Reiher, T. Shiozaki, H. Stoll, A. J. Stone, R. Tarroni, T. Thorsteinsson, and M. Wang. Molpro, version 2012.1.28, a package of ab initio programs, 2012. see, http://www.molpro.net.

[51] R. H. West, G. J. O. Beran, W. H. Green, and M. Kraft. First-principles thermochemistry for the production of TiO_2 from $TiCl_4$. *J. Phys. Chem. A*, 111(18):3560–3565, 2007. doi:10.1021/jp0661950.

[52] R. H. West, M. S. Celnik, O. R. Inderwildi, and M. Kraft. Toward a comprehensive model of the synthesis of TiO_2 particles from $TiCl_4$. *Ind. Eng. Chem. Res.*, 46(19): 6147–6153, 2007. doi:10.1021/ie0706414.

[53] R. H. West, R. A. Shirley, M. Kraft, C. F. Goldsmith, and W. H. Green. A detailed kinetic model for combustion synthesis of titania from $TiCl_4$. *Combust. Flame*, 156 (9):1764–1770, 2009. doi:10.1016/j.combustflame.2009.04.011.